Hindawi
Journal of Engineering
Volume 2024, Article ID 2995863, 13 pages
https://doi.org/10.1155/2024/2995863

Research Article

Effect of an Exhaust Heat Exchanger with Inserts on the Performance of Thermoelectric Generators

Dipak S. Patil and Himadri Majumder

Department of Mechanical Engineering, G H Raisoni College of Engineering and Management, Wagholi, Pune 412207, India

Correspondence should be addressed to Dipak S. Patil; dspatil100@gmail.com

Received 15 November 2023; Revised 8 January 2024; Accepted 19 January 2024; Published 2 February 2024

Academic Editor: Samuel E. Sanni

A thermoelectric generator is used as a waste heat recovery system for generating electric power. The thermoelectric generator system consists of an exhaust heat exchanger, a thermoelectric module, and a water heat exchanger. The aim of the current work is to explore different types of inserts used in the test section of the exhaust heat exchanger and power generation of thermoelectric generators at different operating conditions. An experimental setup has been developed for conducting experimental investigation on thermoelectric generators to find the effect of the exhaust heat exchanger (EHE) with inserts on the performance of thermoelectric generators. The cone (G-type test section) and cone-cylinder (H-type test section) type inserts were introduced to enhance the performance of the thermoelectric generator. Compared with an insert-free (empty, F-type) thermoelectric generator with cone and cone-cylinder type inserts in terms of the output power, the average heat transfer rate and convection heat transfer coefficient of F-type, G-type, and H-type test sections of the EHE are 358, 468, and 459 W and 76, 100, and 97 W/m^{2}K, respectively. It shows that the G-type test section of EHE exchanges more heat from engine exhaust to the hot surface of the thermoelectric module through the wall of the EHE. The G-type test section created more temperature difference; obviously, it generated more power output. It was observed that the G-type and H-type test sections of exhaust heat exchangers improved average maximum output power by 29.49% and 26.11% than that by the F-type test section of heat exchanger, respectively. The F-type, G-type, and H-type test sections of exhaust heat exchangers showed a maximum average efficiency of 0.80, 0.78, and 0.70%, respectively.

1. Introduction

Waste heat is nothing but heat generated with the aid of a method of petroleum/gasoline combustion to dump into the atmosphere and is not used again for beneficial functions. If the waste heat may be recuperated, a notable amount of fuel may be stored [1]. It has been diagnosed that waste heat recuperation technology may be utilized to store the energy [2]. If the part of unwanted heat energy may be recuperated, energy performance could be enhanced and automobiles can save energy and decrease worldwide global warming [3]. A waste heat restoration technology facilitates the regulation of engine temperature [4]. Based on exhaust temperature, bottoming cycle, unique heat exchanger, thermoelectric system, and turbocharger can be hired to recover waste heat [1, 5, 6]. The mechanical or electrical energy can be generated by using high levels of temperature, and the low level temperature can be utilized for water or area heating. The waste heat restoration techniques should be selected according to the temperature condition [7]. Engine producers have accelerated engine efficiency by means of enforcing exclusive strategies such as superior gas/air mixing, turbocharging, and variable valve timing [8]. It is observed that only 5-6% exhaust heat is transferred into electrical energy, and it is shown to save 10% fuel due to reduction in mechanical losses of alternator drive [9]. Fuel reduction depends on heat recovery technologies and the driving cycle [10]. The transformation of temperature difference to an electrical energy or vice versa is known as thermoelectric effect (TEE). Thermoelectric systems are small in size, have no fluid for process, are lightweight, and have no moving parts [11]. Thermoelectric systems have some restrictions, which are high cost and low efficiency; it restricts space, military, and medical uses [12, 13]. Thermoelectric generator (TEG) applications are moved from the most primitive use on a kerosene lamp to medical services, temperature measuring and detecting facilities, aerospace applications, and electronic devices [12]. Thermoelectric systems can be utilized as power generators, thermal sensors, or coolers and are extensively utilized in biology, equipment, and engineering products [11]. The thermoelectric generators are an alternative source to convert solar power into electric power apart from photovoltaic technology [14]. Thermoelectric generators are also utilized in different types of wood stove to produce electric power for lights and to power fans [15–17]. The researchers are concentrating on the design and development of thermoelectric generator systems and heat exchangers. New TEG parameters such as the number of TE modules, cooling system, heat exchanger, and the thermoelectric material should be optimized. [18]. Heat exchangers (HE) supply preliminary heat for a TEG, and its efficiency and capacity are affected by the heat exchanger material [19, 20]. Exhaust thermoelectric generators (ETEGs) can enhance the fuel economy of an engine. The performance of the TEG is affected by heat capacity and heat transfer of the heat recovery device. More thermoelectric modules are required for increasing the output power of the TEG, which requires more surface area. So the weight and size of heat exchangers have increased. The optimization of the heat exchanger surface area is a different kind of issue unlike internal structures [21]. The conversion efficiency and power output of the TEG are significantly affected by the heat source temperature and the mass flow rate of the fluids [22]. Shengqiang Bai et al. [19] developed a heat exchanger with different internal structures such as inclined plate, parallel plate, separate plate with holes, series plate, and novel pipe structures. The plain and offset strip fins were studied by S. Vale et al. [23] with fin dimensions such as length, spacing, height, and thickness. X. Liu et al. [24] performed CFD simulation and analysis of heat exchangers with chaos shape and fishbone shape structures. C. Q. Su et al. [21] tried to achieve a higher temperature at the interface and uniform temperature distribution through different types of internal structures such as fishbone, scatter, and accordion shape. Heat exchange with a symmetrical dimple arrangement in the upper and lower surfaces of the heat exchanger was developed by Yiping Wang et al. [25] to improve the rate of heat transfer with low drop in pressure. The inserted fins deteriorate the emission performance, fuel economy, and performance of the internal combustion engine [26]. This is useful for the enhancement of the hot side temperature of thermoelectric modules and the increment of output power of the automobile exhaust thermoelectric generator [27, 28]. The temperature distribution, temperature uniformity, conversion efficiency, and back pressure should be considered to design the optimization objective, length, width, angle, and spacing of fins inserted inside the heat exchanger [29].

The above survey shows that the TEG is used for heat recovery from engine exhaust. Different types of insert can be used to enhance the performance of exhaust heat exchangers with allowable pressure drop and obviously enhance the performance of the TEG. Selection of the thermoelectric module (TEM) is based on available temperature. The mass flow rate and temperature of both hot and cold fluids govern the thermoelectric power output.

2. Theoretical Analysis

The temperature difference at cold and hot sides of the thermoelectric material generates electrical energy by producing holes and free electrons in the semiconductors and is called as the Seebeck effect. Figure of merit is a method used to measure a thermoelectric performance. High figure of merit can be obtained when the Seebeck coefficient is more and electric resistivity and thermal conductivity are less. The thermoelectric properties such as the Seebeck coefficient, material resistance, and thermal conductance are needed to evaluate the thermoelectric module performance, but they are not available easily to the end user. The thermoelectric properties can be determined from the geometric data of the thermoelectric module such as the number of thermocouples, length, and cross-sectional area of thermocouple. A real TEG consists of a number of thermoelectric elements. Heat conduction loss and Joule electrical resistive loss of cold and hot junctions of the semiconductors are responsible for creating internal irreversibility. The internal heat is created by Joule heat loss I^2R, where I and R are the current and internal resistance, respectively. $K(T_W - T_C)$ is the heat loss by conduction, where K, T_C, and T_W are the heat conductance, cold junction, and hot junction temperature, respectively [30].

The finite rate heat transfer creates external irreversibility, i.e., the temperature differences $(T_C - T_W)$ and $(T_H - T_W)$. Also, $k_C A_C$ and $k_H A_H$ are the heat conductance in the cold and hot sides of HE, where A_H and k_H are the hot side HE area and heat transfer coefficient for thermoelectric element and A_C and k_C are the cold side heat exchanger area and heat transfer coefficient for thermoelectric element. Therefore, the heat transfer rate from the heat source to the element hot end at temperature, and the heat transfer rate from the element cold end at temperature to the heat sink [31].

$$\begin{aligned} Q_H &= \left[\alpha \mathrm{I}T_W - 0.5\mathrm{RI}^2 + K\left(T_W - T_C\right)\right] \\ &= \left(k_H A_H\right)\left(T_H - T_W\right), \\ Q_L &= \left[\alpha I T_C - 0.5\mathrm{RI}^2 + K\left(T_W - T_C\right)\right] \\ &= \left(k_C A_C\right)\left(T_C - T_C\right), \end{aligned} \tag{1}$$

where $\alpha = \alpha_P - \alpha_N$, α_N, and α_P are the coefficients of Seebeck of the N-type and P-type semiconductor legs.

A practical TEG consists of n number of thermoelectric elements. Therefore, the rate of absorbing heat becomes nQ_H and the rate of rejecting heat is nQ_L.

Where $(k_C A_C)$ and $(k_H A_H)$ are the heat conductance of exchangers between the TEG cold and hot nodes, adding above equations yields

$$T_W = \left[\left(\frac{k_H A_H T_H}{n} + 0.5\mathrm{RI}^2\right)\left(\frac{k_C A_C}{n} + \alpha I\right) + K\left(\frac{k_H A_H T_H}{n}\right) + \left(\frac{k_C A_C T_L}{n}\right) + I^2 R \times \left(\left(\frac{k_H A_H}{n} + \alpha I\right)\left(\frac{K_C A_C}{n} - \alpha I\right) + K\left(\frac{k_H A_H + K_C A_C}{n}\right)\right)^{-1}\right],$$

$$T_C = \left[\left(\frac{K_C A_C T_L}{n} + 0.5RI^2\right)\left(\frac{k_H A_H}{n} + \alpha I\right) + K\left(\frac{k_H A_H T_H}{n} + \frac{K_C A_C T_L}{n} + I^2 R\right) \times \left(\left(\frac{k_H A_H}{n} + \alpha I\right)\left(\frac{k_C A_C}{n} - \alpha I\right) + K\left(\frac{k_H A_{H+k_C A_C}}{n}\right)\right)^{-1}\right],$$

$$Q_H = k_H A_H \left\{\frac{\alpha \mathrm{RI}^3}{2} - I^2\left[\frac{T_H \alpha^2 + k_C A_C R}{(2n) + \mathrm{KR}}\right] + \frac{I k_C A_C T_H \alpha}{n} + \frac{K k_C A_C (T_H - T_L)}{n}\right\} \times \left(\left(\frac{k_H A_H}{n} + \alpha I\right)\left(\frac{k_C A_C}{n} - \alpha I\right) + \left(K\frac{(k_H A_H + K_C A_C)}{n}\right)\right)^{-1}\right),$$

$$\begin{aligned} Q_L = k_C A_C &\left\{\frac{\alpha \mathrm{RI}^3}{2} - I^2\left[\frac{T_L \alpha^2 + k_H A_H R}{(2n)} + \mathrm{KR}\right] + \frac{I k_H A_H T_L \alpha}{n} + \frac{K k_H A_H (T_H - T_L)}{n}\right\} \\ &\times \left(\left(\frac{k_H A_H}{n} + \alpha I\right)\left(\frac{k_C A_C}{n} - \alpha I\right) + n\left(K\frac{(k_H A_H + K_C A_C)}{n}\right)\right)^{-1}. \end{aligned} \tag{2}$$

Here, P is output power and η is the conversion efficiency of the TEG:

$$\begin{aligned} P &= Q_H - Q_L, \\ \eta &= \frac{Q_H - Q_L}{Q_L} \\ &= 1 - \left(\frac{Q_L}{Q_H}\right). \end{aligned} \tag{3}$$

Combining above equations gives

$$\begin{aligned} P = &\left(I^3 \frac{(k_H A_H - k_C A_C) R\alpha}{2I^2}\right)\left[(k_H A_H T_H - k_C A_C T_L)\alpha^2 + \frac{k_H A_H k_C A_C R}{n}(k_H A_H + k_C A_C)\mathrm{KR}\right] + \left(\frac{\mathrm{I} k_H A_H k_C A_C \alpha (T_H - T_L)}{n}\right) \\ &\times \left(\left(\frac{k_H A_H}{n} + \alpha I\right) + K\frac{(k_H A_H + k_C A_C)}{n}\right)^{-1}, \end{aligned} \tag{4}$$

$$\begin{aligned} \eta = &\left(I^3 \frac{(k_H A_H - k_C A_C) R\alpha}{2I^2}\left[(k_H A_H T_H - k_C A_C T_L)\alpha^2 + \frac{k_H A_H k_C A_C R}{n} + (k_H A_H + k_C A_C)\mathrm{KR}\right] + \frac{\mathrm{I} k_H A_H k_C A_C \alpha (T_H - T_L)}{n}\right) \\ &\times \left(k_H A_H \left\{\frac{I^3 R\alpha}{2} - I^2\left[\frac{T_H \alpha^2 + k_C A_C R}{(2n)} + \mathrm{KR}\right] + \frac{\mathrm{I} k_C A_C T_H \alpha}{n} + \frac{K k_C A_C (T_H - T_L)}{n}\right\}\right)^{-1}. \end{aligned} \tag{5}$$

Equations (4) and (5) show heat reservoir temperatures effects (T_H and T_L), heat transfers ($k_H A_H$ and $k_C A_C$), internal resistance (R), internal heat conductance (K), current $(I)\lim_{x \longrightarrow \infty}$, coefficient of Seebeck (α), and number of thermoelectric elements (n) on the power output (P) and efficiency (η) of the TEG.

When $n = 1$, equations (4) and (5) become the finite time analysis results of single element of the TEG. If $k_H A_H = k_C A_C \longrightarrow \infty$, $T_W = T_H$, and $T_C = T_L$, equations (4) and (5) become the results of nonequilibrium thermodynamic analysis.

$$\begin{aligned} P &= \left[\alpha (T_H - T_L) I - I^2 R\right] n, \\ \eta &= \frac{\alpha (T_H - T_L) I - I^2 R}{\alpha T_H I - 0.5RI^2 + K(T_H - T_L)}. \end{aligned} \tag{6}$$

In this case, η is independent on n and P is dependent on n. If $n = 1$, equation (6) become the results of reference. However, $T_W = T_H$ and $T_C = T_L$ need infinite surface area of heat transfer, and its specific output power $P/(A_H + A_C)$ is zero.

3. Experimental Details

3.1. Thermoelectric Generator (TEG) System. The heat recovery from the engine exhaust with the help of an exhaust heat exchanger and the engine specification is shown in Table 1. The exhaust heat exchanger (EHE) is a main component of thermoelectric generators. It is divided into three parts, namely, the front part, middle part, and rear part. The front part has 38 mm diameter at the entry end and 60×60 mm cross-section at the exit end with a length of 150 mm. The rear part is the same as the front part but the direction is opposite to the front part. The middle part of the EHE has a $60 \times 60\ \mathrm{mm}^2$cross-section on both sides with a length of 180 mm. The middle part of EHE is called the test section. The front and rear parts of EHE are made up of mild steel (MS) with a thickness of 5 mm. The test section of EHE is made up of Al (aluminum) material with a thickness of 3 mm. The front, rear, and middle parts of EHE are shown in Figure 1. All the parts of EHE having flanges at both ends are used to connect each other by fasteners. The EHE is joined to the exhaust pipe of an engine. The EHE absorbs heat energy from the engine exhaust to maintain high temperature at all surfaces. The water heat exchanger (WHE) is equally important as an exhaust heat exchanger, as shown in Figure 2. It is a simple box of 40 mm width, 160 mm length, and 15 mm height and is made up of an aluminum sheet of 3 mm thickness. The water heat exchanger contains six numbers of baffles of $3 \times 15 \times 30$ mm (thick × height × length) size for guiding zigzagging to cold fluid. Water was used as a cooling fluid to maintain low temperature at the cooling side of the thermoelectric module (TEM). The WHE has an entry and exit port of 5 mm diameter. There are four numbers of water heat exchangers used in the TEG. The various types of inserts can be used to improve the temperature uniformity coefficient and surface temperature of the test section. The inserts are shown in Figure 3, namely, the cone type (G-type) and con-cylinder type (H-type). The EHE without insert is known as F-type HE. All the inserts are made up of a tin sheet of 2 mm thickness. The size of the cone type insert is a base diameter of 46.5 mm with a length of 180 mm. The cone-cylinder type insert is a combination of cone and cylinder of 46.5 mm diameter with a length of 90 mm each. The TEM is the heart of the TEG; its semiconducting material shows low thermal conductivity and high electric conductivity. The thermoelectric material (TM) converts heat energy to electric energy by using the Seebeck effect. In this work, bismuth telluride (TEP1-1264-1.5) thermoelectric modules were used. The size of the TEM is $40 \times 40 \times 3.5$ mm; the detailed specification is shown in Table 2. The TEM consists of a number of thermocouples (N-type and P-type) that are thermally connected in parallel and electrically in series. All the thermocouples of TEM are sandwiched between ceramic plates. It is very important to identify cold and hot sides of the TEM as displayed in Figure 4. The inserts play a vital role in enhancing surface temperature distribution and temperature uniformity coefficient. The inserts direct the engine exhaust in such a way to increase surface temperature of the exhaust heat exchanger. The G- and H-type test sections show high temperature uniformity coefficients of 0.94 and 0.96. The permissible pressure drop has been created on the engine by using the inserts. Hybrid type inserts can be used to recover the waste heat from the engine exhaust by caring for back pressure, temper uniformity, and surface temper of the exhaust heat recovery system.

3.2. Experimental Setup. The experimental setup was developed to perform the experimental investigation on the TEG under different operating conditions. Figure 5(a) shows the experimental system of the TEG. Four numbers of thermoelectric modules (TEMs) are located over all (four) surfaces of the EHE. The water heat exchanger (WHE) was located over the thermoelectric modules at each surfaces of the EHE. All the TEMs were serially connected to each other. The EHE, WHE, and TEMs are fixed by the "C" clamp. The entire assembly of the TEG was connected at the exhaust pipe of the engine. The water system was linked with the WHE of the TEG. All the thermocouples are fixed at the appropriate places on the thermoelectric generator for measuring the temperature of the inlet and outlet of water and engine exhaust and cold and hot sides of the thermoelectric modules. The thermocouples are connected with a temperature meter. The ball and gate valves are connected in the lane of water and the exhaust flow to control the water and exhaust flow rates. The manometer was coupled at the exhaust inlet and outlet of the TEG to measure the pressure drop. The multimeter and preset were linked with thermoelectric modules. The schematic layout and photographs of the experimental setup are shown in Figures 5(b) and 5(c), respectively.

3.3. Operating Conditions. The different operating conditions should be fixed before performing the experiment on the thermoelectric generators. The parameters and their levels considered for experimentations are shown in Table 3. The first factor was the test section of the exhaust heat exchanger (EHE) of $60 \times 60 \times 180$ mm with and without an insert. It has three levels; the first test section without an insert is named F-type, the second test section with a cone type insert is named G-type, and the third test section with a cylinder-cone type insert is named H-type. The second factor was the engine load (EL) which has six levels of 0, 2, 4, 6, 8, and 10 kg. The engine load can be applied or control by an electric (eddy current) dynamometer which is connected to the engine shaft. The third factor was the water flow rate (WFR) of 0.030, 0.050, and 0.080 kg/s. The flow control system consists of two ball valves to regulate the mass flow rate of fluid. One of the valves was fixed in the path of the cooling water supply to bypass the excess amount of water, and another valve was used to control/regulate the water mass flow rate of the water heat exchanger. The last factor was external load resistance (ELR) of 0–50 Ω with 5 Ω increments and 50–100 Ω with 10 Ω increments. According to the factors and their levels, the experiments were carried out

Table 1: Engine specification.

Particular	Specification
Number of cylinder	Single
Engine stroke	Four
Fuel	Diesel
Engine power	3.5 kW
Engine speed	1500 rpm (constant speed)
Cylinder stroke length	110 mm
Bore diameter	87.5 mm
Engine capacity	661 cc
Compression ratio	17.5 : 1

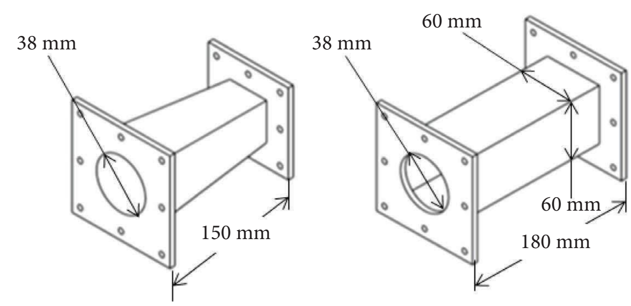

Figure 1: Front/rear and middle parts of the exhaust heat exchanger (EHE).

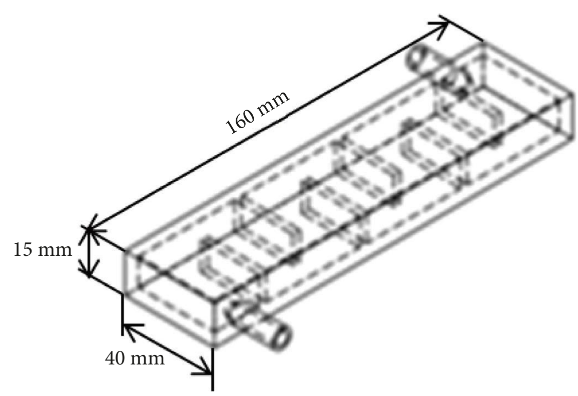

Figure 2: Water heat exchanger (WHE).

on the thermoelectric generator system. The total number of trials were 864 which have been performed on the experimental setup. The exhaust entry and exit temperature, water entry and exit temperature, WFR, cold and hot side temperature of TEMs, manometer reading, and thermoelectric voltage and current were measured. The thermoelectric output power is a multiplication of thermoelectric current and voltage. All the observations were taken for F-type, G-type, and H-type test sections of the exhaust heat exchanger under different engine loads of 0, 2, 4, 6, 8, and 10 kg, water flow rates of 0.030, 0.050, and 0.080 kg/s, and an external load resistance of 0, 5, 10, 15, . . ., 50, 60, . . ., and 100 Ω.

4. Results and Discussion

The experiment has been conducted on the thermoelectric generator by using different test sections of F-type, G-type, and H-type while changing the engine load, water flow rate, and ELR. The engine exhaust was considered as air; the properties of air are assessed at the mean temperature. The engine exhaust was selected as the heat source and water as the heat sink. The bismuth telluride thermoelectric modules (TEP1-1264-1.5) were used for the thermoelectric generator. The performance of the TEG was measured in terms of thermoelectric voltage, current, and output power. The different types of test section of the heat exchanger, WFR, EL, and ELR are the parameters of an experimental investigation. The aim of the current work is to search different types of inserts used in the test section of the EHE and power generation of TEGs at different operating conditions. The average heat transfer rate and convection heat transfer coefficient of F-type, G-type, and H-type test sections of the exhaust heat exchanger are 358, 468, and 459 W and 76, 100, and 97 W/m^2K, respectively. It shows that the G-type test section of the exhaust heat exchanger exchanges more heat from the engine exhaust to the hot surface of the thermoelectric module through the wall of the exhaust heat exchanger. The G-type test section created more temperature difference; obviously, it generated more power output.

4.1. Effect of External Load Resistance (ELR) on Voltage, Current, and Output Power. The thermoelectric voltage, current, and output power variation of the F-type, G-type, and H-type test sections of the EHE with ELR (0–100 Ω) at EL of 10 kg and different WFR (0.03, 0.05, and 0.08 kg/s) are shown in Figures 6–8. The thermoelectric voltage increases with increasing ELR. The thermoelectric current decreases with increasing ELR. The thermoelectric output power increases with increasing ELR; once it has achieved maximum output power, it then decreases with increasing ELR. The maximum thermoelectric output power is obtained when ELR matches with the internal resistance and is called matched load output power. The G-type test section of the exhaust heat exchanger shows higher voltage, current, and output power than other test sections. The F-type test section of the EHE generated the maximum output power of 3.80, 3.92, and 4.30 W at WFR of 0.03, 0.05, and 0.08 kg/s, respectively, EL of 10 kg, and ELR of 40 Ω, as shown in Figure 6. Similarly, the G-type and H-type test sections of EHE generated the output power of 4.79, 5.24, and 5.59 W and 4.21, 4.51, and 4.83 W at WFR of 0.03, 0.05, and 0.08 kg/s, respectively, EL of 10 kg, and ELR of 45 Ω, as shown in Figures 7 and 8. The G-type and H-type test sections of the exhaust heat exchanger improved the average maximum output power by 29.49% and 26.11% than that by the F-type test section of the heat exchanger, respectively. Thermoelectric voltage generation depends on temperature difference between hot and cold surfaces of the thermoelectric modules. The G-type (cone) test section maintained more temperature difference and generated more voltage and power output than H-type (cone–cylinder) and F-type (empty) test sections. The matched load condition shows maximum thermoelectric power generation. Thermoelectric current decreases with increasing external load resistance.

Cone type insert Cone-Cylinder type insert

Figure 3: Photos of different types of inserts.

Table 2: Description of the TEM 1 (TEM1).

TEM	Model dimension (mm)	Parameters	Value
TEP1-1264-1.5	$40 \times 40 \times 3.5$	Temperature (°C) (hot side)	300
		Temperature (°C) (cold side)	30
		Open circuit voltage (V)	9.40
		Resistance (Ohms) (matched load)	2.80
		Output voltage (V) (matched load)	4.70
		Output current (A) (matched load)	1.56
		Output power (W) (matched load)	7.30

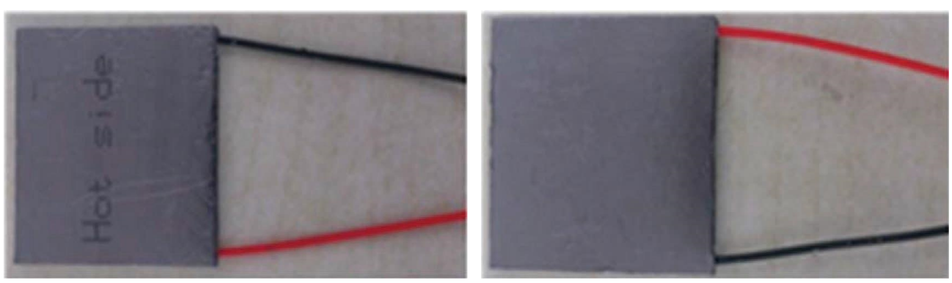

Figure 4: Hot and cold sides of the thermoelectric module ($40 \times 40 \times 3.5$ mm).

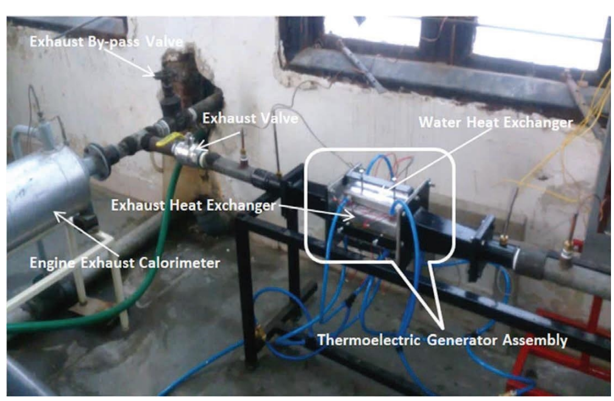

(a)

Figure 5: Continued.

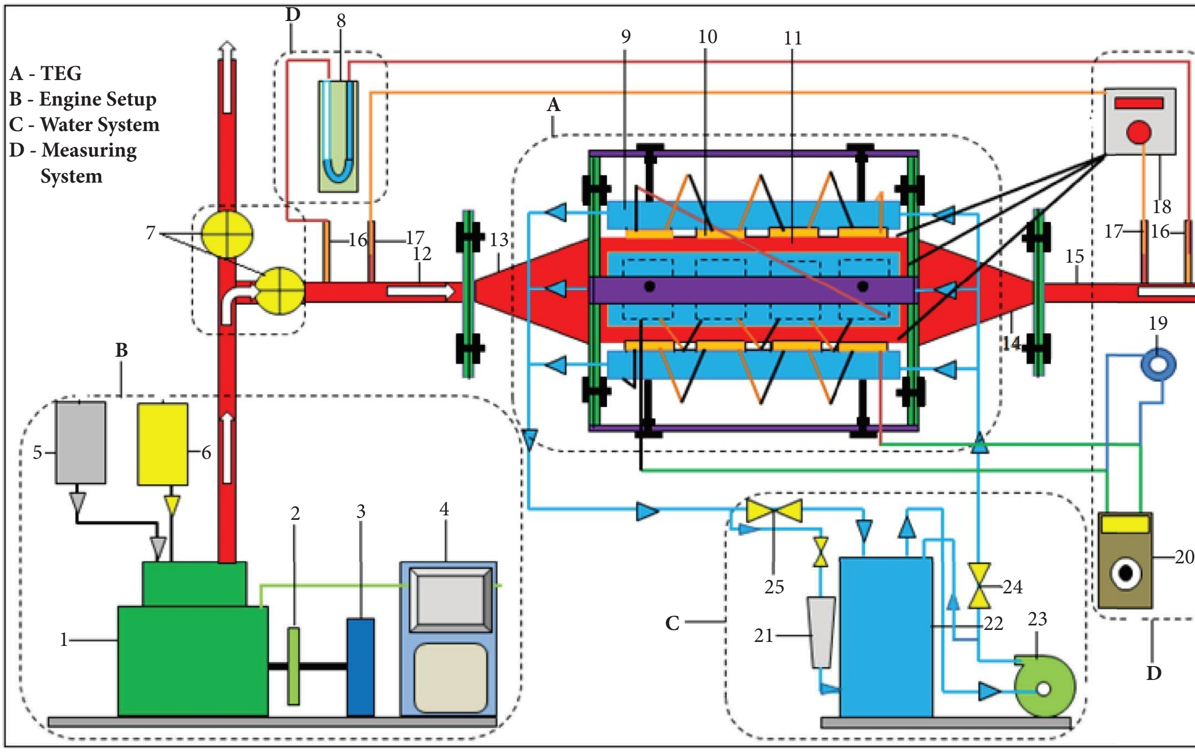

1-Engine setup, 2- Engine flywheel, 3-Dynamo meter, 4- Data storage system, 5- Air box, 6- Diesel tank, 7-Exhaust control valves, 8- U tube manometer, 9-Heat sink (water heat exchanger (WHE)), 10- Thermoelectric module, 11-Heat source (exhaust heat exchanger (EHE)), 12- Inlet of EHE, 13- Front part of EHE, 14- Rear part of EHE, 15- Outlet of EHE, 16- U tube manometer connectors, 17-Thermocouples for inlet and outlet exhaust temperature, 18- Temperature meter, 19- Preset, 20- Multi-meter, 21- fluid flow measuring flask, 22- Water tank, 23- Self-priming pump, 24- Water inlet flow control valves, 25- Water outlet flow control valves

(b)

(c)

Figure 5: (a) Experimental setup of the thermoelectric generator. (b) Schematic layout of the experimental setup. (c) Photographs of the experimental setup.

Table 3: Parameters for experimentation.

S.n.	Factors	Levels								
1	Test section of EHE (with/without insert)	F-type (empty type, without insert)	G-type (cone type insert)	H-type (cone-cylinder type insert)						
2	Engine load (EL), kg	0	2	4	6	8	10			
3	Water flow rate (WFR), kg/s	0.030	0.050	0.080						
4	External load resistance (ELR), Ω	0	5	10	15	...	50	60	...	100

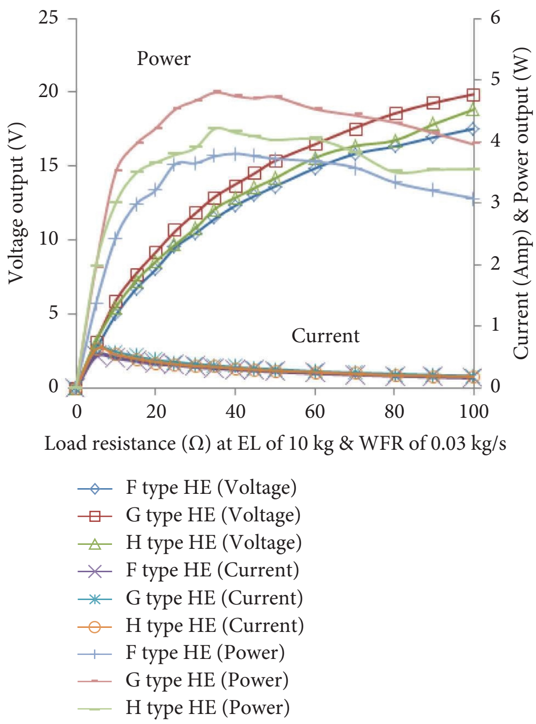

FIGURE 6: Voltage, current, and power output variation of the F-type, G-type, and H-type heat exchangers with load resistance at EL 10 kg and WFR 0.03 kg/s.

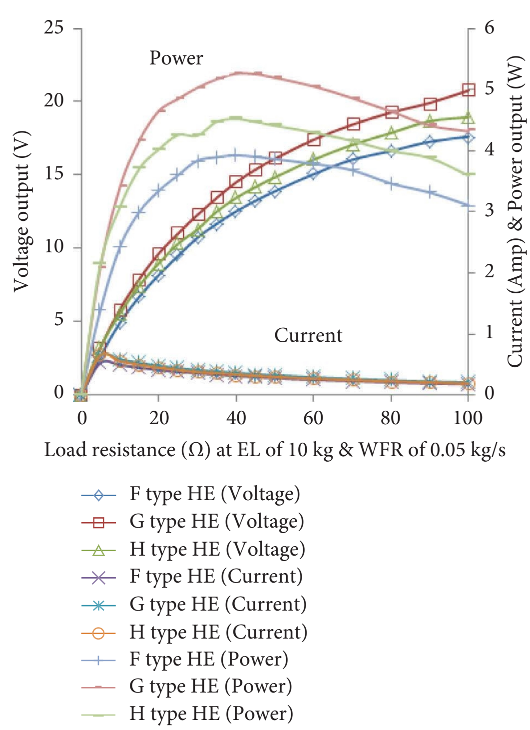

FIGURE 7: Voltage, current, and power output variation of the F-type, G-type, and H-type heat exchangers with load resistance at EL 10 kg and WFR 0.05 kg/s.

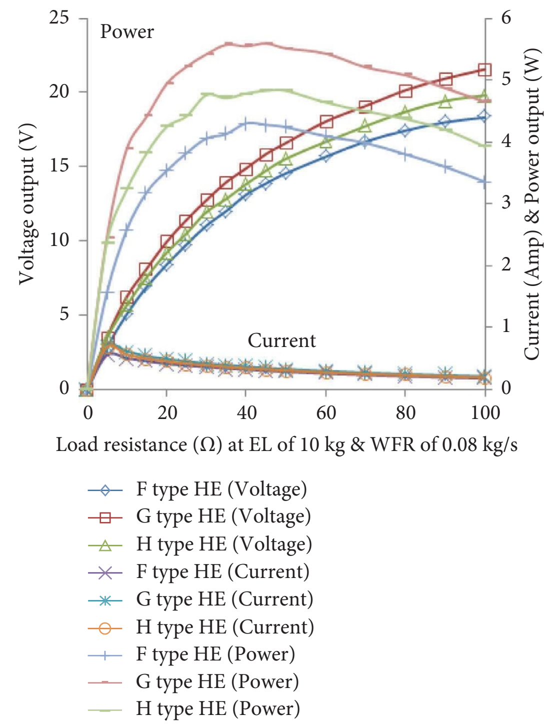

FIGURE 8: Voltage, current, and power output variation of the F-type, G-type, and H-type heat exchangers with load resistance at EL 10 kg and WFR 0.08 kg/s.

4.2. Validation of Experimental TEG Power Output with the Theoretical Model of TEM. The theoretical and experimental output power increases with increasing hot surface temperature of the TEM. The difference between theoretical and experimental power outputs at lower temperature of the hot surface is very less but it increases with increasing the hot surface temperature. The theoretical power output range of F-type, G-type, and H-type test sections are 0.46–4.65 W, 0.75–6.29 W, and 0.64–5.74 W, respectively. The experimental power output range of F-type, G-type, and H-type test sections is 0.38–4.80 W, 0.71–5.59 W, and 0.62–4.83 W, respectively, as shown in Figure 9. The average error between theoretical and experimental power outputs of F-type, G-type, and H-type EHE is 10.90%, 11.60%, and 14.10%, respectively.

4.3. Effect of External Load Resistance (ELR) on Thermoelectric Efficiency. The thermoelectric efficiency variation of the F-type, G-type, and H-type test sections of the EHE with ELR (0–100 Ω) at EL of 10 kg and different WFRs (0.03, 0.05, and 0.08 kg/s) is shown in Figures 10–12. The thermoelectric efficiency increases with increasing ELR; once it has achieved maximum efficiency, it then decreases with increasing ELR. The F-type test section of EHE showed the maximum efficiency of 0.76, 0.78, and 0.86% at WFR of 0.03, 0.05, and 0.08 kg/s, respectively, EL

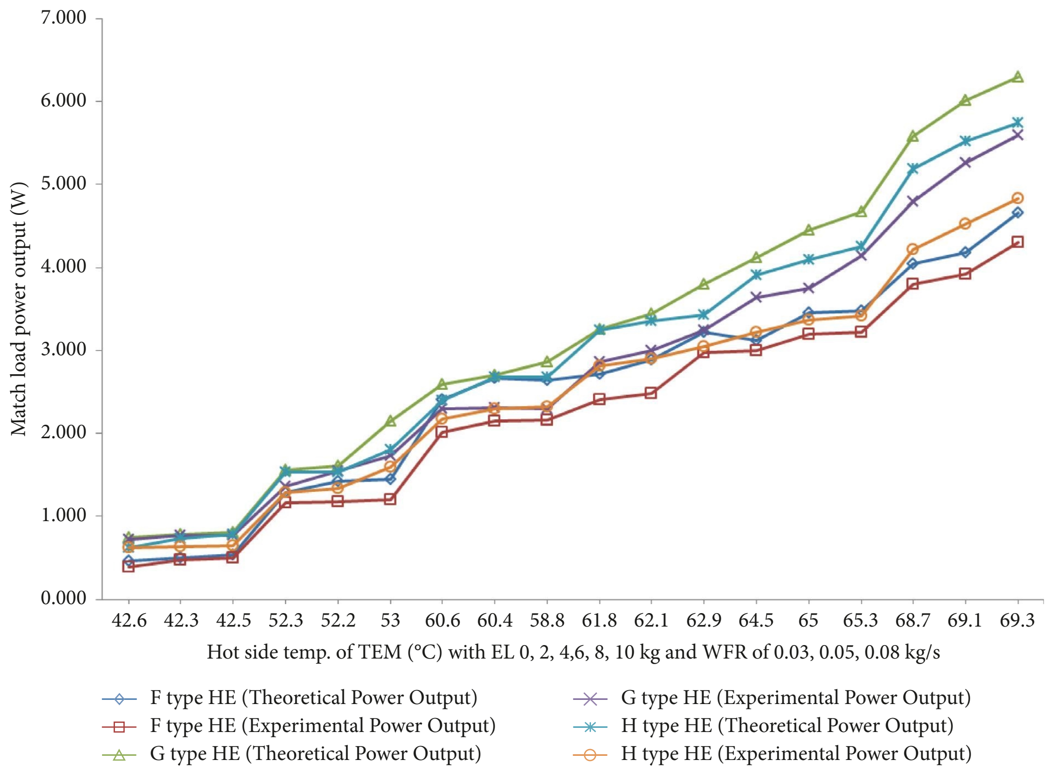

Figure 9: Comparison of experimental output power with theoretical power output for F-type, G-type, and H-type HE.

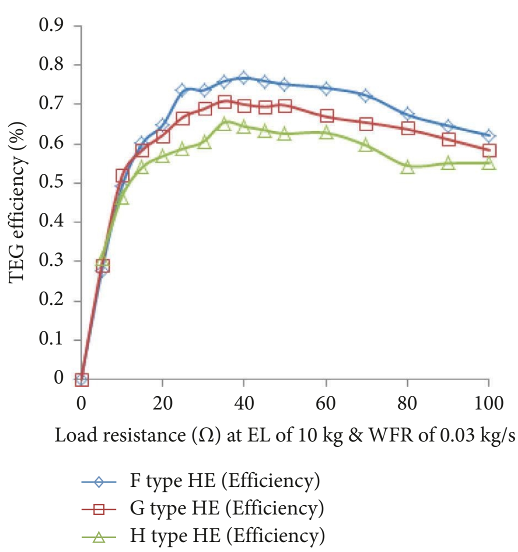

Figure 10: Thermoelectric efficiency variation of the F-type, G-type, and H-type heat exchangers with load resistance at EL 10 kg and WFR 0.03 kg/s.

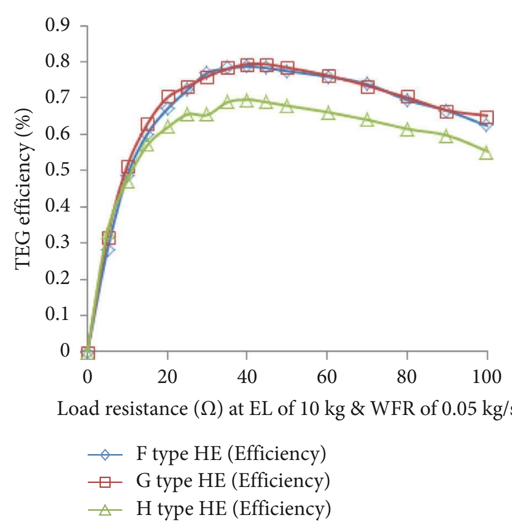

Figure 11: Thermoelectric efficiency variation of the F-type, G-type, and H-type heat exchangers with load resistance at EL 10 kg and WFR 0.05 kg/s.

of 10 kg, and ELR of 40 Ω. Similarly, the G-type and H-type test sections of EHE showed the maximum efficiencies of 0.70, 0.79, and 0.84% and 0.65, 0.69, and 0.75% at WFR of 0.03, 0.05, and 0.08 kg/s, respectively, EL of 10 kg, and ELR of 40–45 Ω. The F-type, G-type, and H-type test sections of the exhaust heat exchanger showed maximum average efficiencies of 0.80, 0.78, and 0.70%, respectively.

4.4. Pressure Drop. The variation of exhaust pressure drop of all test sections with engine load is shown in Figure 13. The exhaust pressure drop of all test sections increases with increasing the engine load. The ranges of exhaust pressure drop of F-type, G-type, and H-type test sections show 853–1207, 903–1256, and 952–1285 Pa, respectively. It reflects that the H-type test section shows more pressure drop and the F-type test section shows minimum pressure drop. Intermediate pressure drop is shown by the G-type test section.

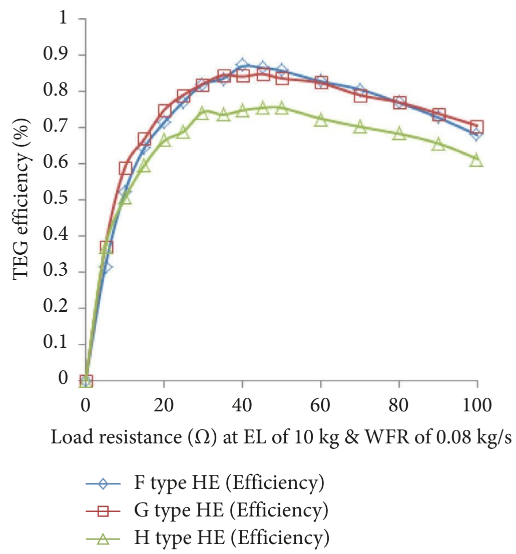

FIGURE 12: Thermoelectric efficiency variation of the F-type, G-type, and H-type heat exchangers with load resistance at EL 10 kg and WFR 0.08 kg/s.

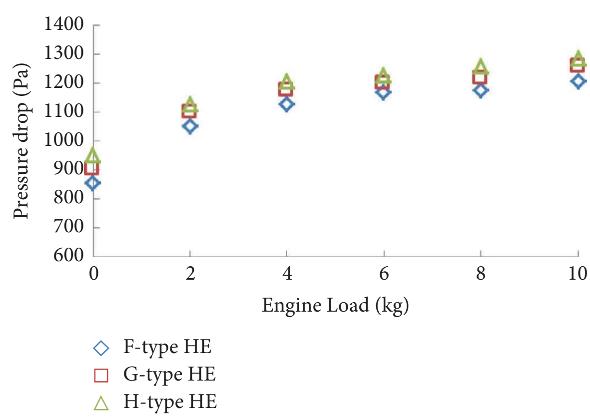

FIGURE 13: Pressure drop of F-type, G-type, and H-type heat exchangers with engine loads.

5. Conclusions

The parameters of the study are heat exchangers with different kinds of inserts, water flow rate of the water heat exchanger, engine load, and external load resistance. Results are generated in the form of the thermoelectric voltage, current, and output power. The G-type test section of the exhaust heat exchanger extracted more heat compared to the F-type and H-type test sections. The output power increases with increasing EL 0–10 kg and the water flow rate of 0.03–0.08 kg/s. The F-type test section of the exhaust heat exchanger generated the maximum power output of 4.30 W at the engine load of 10 kg, water flow rate of 0.08 kg/s, and ELR of 40 Ω. Similarly the G-type and H-type test sections of the exhaust heat exchanger generated the maximum output power of 5.59 W and 4.83 W at the engine load of 10 kg, water flow rate of 0.08 kg/s, and external load resistance of 45 Ω, respectively. The average error between theoretical and experimental power outputs of F-type, G-type, and H-type EHE is 10.90%, 11.60%, and 14.10%, respectively. The G-type and H-type test sections of the exhaust heat exchanger improved maximum output power by 29.49% and 26.11% than that by the F-type test section. The difference between theoretical and experiment output power is due to the effects of heat losses and nonuniform exhaust flow in the thermoelectric generator. The F-type, G-type, and H-type test sections of the exhaust heat exchanger showed maximum average efficiencies of 0.80, 0.78, and 0.70%, respectively. The G-type test section generated a permissible pressure drop. It is observed that the G-type test section is suitable for thermoelectric generators to generate maximum power. In future, different kinds of insert geometries can be designed to absorb maximum amount of heat with allowable pressure drop. The simulation tool should be used to analyze the performance of the heat exchanger with the inserts to save the cost and time.

Nomenclature

I: Electric current, Amp
K: Thermal conductance, WK^{-1}
k: Thermal conductivity, $Wm^{-1}K^{-1}$
P: Power output, W
Q: Heat transfer rate, W
Q_P: Power output, W
T: Temperature, ˚C or K
V: Voltage, V

Greek Symbols

α: Seebeck coefficient, VK^{-1}
η: Efficiency of thermoelectric generator
ΔT: Temperature difference, K or ˚C

Subscripts

$_c$: Cold side, cold junction
$_{\text{Ceramic}}$: Ceramic plate
$_{\text{con}}$: Conversion
$_{\text{Copper}}$: Copper strip
$_{\text{exp}}$: Experiment
$_{\text{Grease}}$: Thermoelectric grease
$_h$: Hot side
$_{\text{in}}$: Input
$_{\text{max}}$: Maximum value
$_{\text{out}}$: Output
$_{\text{solder}}$: Soldering material layer
$_{\text{th}}$: Thermoelectric

Abbreviations

Cu: Copper
EL: Engine load
ELR: External load resistance
ETEG: Exhaust thermoelectric generators
EHE: Exhaust heat exchanger
HE: Heat exchanger
HTC: Heat transfer coefficient (convective)
TEG: Thermoelectric generator
TEM: Thermoelectric module

TM: Thermoelectric material
WFR: Water flow rate
WHE: Water heat exchanger.

Data Availability

The data used to support the findings of the study are available from the corresponding author upon request.

Conflicts of Interest

The authors declare that they have no conflicts of interest.

Acknowledgments

The authors acknowledge the management of G H Raisoni College of Engineering and Management, Wagholi, Pune, India, for providing research laboratories for the research and their support in conducting this work.

References

[1] V. Pandiyarajan, M. Chinna Pandian, E. Malan, R. Velraj, and R. V. Seeniraj, "Experimental investigation on heat recovery from diesel engine exhaust using finned shell and tube heat exchanger and thermal storage system," *Applied Energy*, vol. 88, no. 1, pp. 77–87, 2011.
[2] R. Saidur, M. Rezaei, W. K. Muzammil, M. H. Hassan, S. Paria, and M. Hasanuzzaman, "Technologies to recover exhaust heat from internal combustion engines," *Renewable and Sustainable Energy Reviews*, vol. 16, no. 8, pp. 5649–5659, 2012.
[3] E. H. Wang, H. G. Zhang, B. Y. Fan, M. G. Ouyang, Y. Zhao, and Q. H. Mu, "Study of working fluid selection of organic Rankine cycle (ORC) for engine waste heat recovery," *Energy*, vol. 36, no. 5, pp. 3406–3418, 2011.
[4] P. Kauranen, T. Elonen, L. Wikström, J. Heikkinen, and J. Laurikko, "Temperature optimisation of a diesel engine using exhaust gas heat recovery and thermal energy storage (diesel engine with thermal energy storage)," *Applied Thermal Engineering*, vol. 30, no. 6-7, pp. 631–638, 2010.
[5] V. Dolz, R. Novella, A. García, and J. Sánchez, "HD Diesel engine equipped with a bottoming Rankine cycle as a waste heat recovery system. Part 1: study and analysis of the waste heat energy," *Applied Thermal Engineering*, vol. 36, pp. 269–278, 2012.
[6] S. Zhu, K. Deng, and S. Qu, "Energy and exergy analyses of a bottoming Rankine cycle for engine exhaust heat recovery," *Energy*, vol. 58, pp. 448–457, 2013.
[7] G. Shu, Y. Liang, H. Wei, H. Tian, J. Zhao, and L. Liu, "A review of waste heat recovery on two-stroke IC engine aboard ships," *Renewable and Sustainable Energy Reviews*, vol. 19, pp. 385–401, 2013.
[8] C. Sprouse and C. Depcik, "Review of organic Rankine cycles for internal combustion engine exhaust waste heat recovery," *Applied Thermal Engineering*, vol. 51, no. 1-2, pp. 711–722, 2013.
[9] H. Tian, G. Shu, H. Wei, X. Liang, and L. Liu, "Fluids and parameters optimization for the organic Rankine cycles (ORCs) used in exhaust heat recovery of Internal Combustion Engine (ICE)," *Energy*, vol. 47, no. 1, pp. 125–136, 2012.
[10] A. Legros, L. Guillaume, M. Diny, H. Zaïdi, and V. Lemort, "Comparison and impact of waste heat recovery technologies on passenger car fuel consumption in a normalized driving cycle," *Energies*, vol. 7, no. 8, pp. 5273–5290, 2014.
[11] S. B. Riffat and X. Ma, "Thermoelectrics: a review of present and potential applications," *Applied Thermal Engineering*, vol. 23, no. 8, pp. 913–935, 2003.
[12] R. Yue and J. Xu, "Poly(3,4-ethylenedioxythiophene) as promising organic thermoelectric materials: a mini-review," *Synthetic Metals*, vol. 162, no. 11-12, pp. 912–917, 2012.
[13] D. M. Rowe, "Thermoelectrics, an environmentally-friendly source of electrical power," *Renewable Energy*, vol. 16, no. 1-4, pp. 1251–1256, 1999.
[14] W. He, G. Zhang, X. Zhang, J. Ji, G. Li, and X. Zhao, "Recent development and application of thermoelectric generator and cooler," *Applied Energy*, vol. 143, pp. 1–25, 2015.
[15] D. Champier, J. P. Bedecarrats, M. Rivaletto, and F. Strub, "Thermoelectric power generation from biomass cook stoves," *Energy*, vol. 35, no. 2, pp. 935–942, 2010.
[16] D. Champier, J. P. Bédécarrats, T. Kousksou, M. Rivaletto, F. Strub, and P. Pignolet, "Study of a TE (thermoelectric) generator incorporated in a multifunction wood stove," *Energy*, vol. 36, no. 3, pp. 1518–1526, 2011.
[17] R. Mal, R. Prasad, V. K. Vijay, and A. R. Verma, "The design, development and performance evaluation of thermoelectric generator (TEG) integrated forced draft biomass cook stove," *Procedia Computer Science*, vol. 52, pp. 723–729, 2015.
[18] C.-C. Weng and M.-J. Huang, "A simulation study of automotive waste heat recovery using a thermoelectric power generator," *International Journal of Thermal Sciences*, vol. 71, pp. 302–309, 2013.
[19] S. Bai, H. Lu, T. Wu, X. Yin, X. Shi, and L. Chen, "Numerical and experimental analysis for exhaust heat exchangers in automobile thermoelectric generators," *Case Studies in Thermal Engineering*, vol. 4, pp. 99–112, 2014.
[20] D. S. Patil, R. R. Arakerimath, and P. V. Walke, "Thermoelectric materials and heat exchangers for power generation–A review," *Renewable and Sustainable Energy Reviews*, vol. 95, pp. 1–22, 2018.
[21] C. Q. Su, W. S. Wang, X. Liu, and Y. D. Deng, "Simulation and experimental study on thermal optimization of the heat exchanger for automotive exhaust-based Thermoelectric generators," *Case Studies in Thermal Engineering*, vol. 4, pp. 85–91, 2014.
[22] S. P. Dipak, R. R. Arakerimath, and P. V. Walke, "Experimental investigation and optimization of a low-temperature thermoelectric module with different operating conditions," *World Journal of Engineering*, vol. 16, no. 3, pp. 1–10, 2018.
[23] S. Vale, L. Heber, P. J. Coelho, and C. M. Silva, "Parametric study of a thermoelectric generator system for exhaust gas energy recovery in diesel road freight transportation," *Energy Conversion and Management*, vol. 133, pp. 167–177, 2017.
[24] X. Liu, Y. D. Deng, K. Zhang, M. Xu, Y. Xu, and C. Q. Su, "Experiments and simulations on heat exchangers in thermoelectric generator for automotive application," *Applied Thermal Engineering*, vol. 71, no. 1, pp. 364–370, 2014.
[25] Y. Wang, S. Li, X. Yang, Y. Deng, and C. Su, "Numerical and experimental investigation for heat transfer enhancement by dimpled surface heat exchanger in thermoelectric generator," *Journal of Electronic Materials*, vol. 45, no. 3, pp. 1792–1802, 2016.
[26] R. Quan, Y. Li, T. Li, Y. Chang, and H. Yan, "Numerical and experimental study on performance of a low-backpressure

polyhedral thermoelectric generator for waste heat recovery," *Journal of Thermal Science*, vol. 32, no. 1, pp. 109–124, 2023.
[27] R. Quan, W. Liang, S. Quan et al., "Performance interaction assessment of automobile exhaust thermoelectric generator and engine under different operating conditions," *Applied Thermal Engineering*, vol. 216, pp. 119055–119115, 2022.
[28] R. Quan, J. Wang, W. Liang, X. Li, and Y. Chang, "Numerical investigation of a thermoelectric generator system with embedded sickle-shaped fins," *Applied Thermal Engineering*, vol. 236, pp. 121741–121819, 2024.
[29] R. Quan, H. Guo, D. Liu, Y. Chang, and H. Wan, "Performance optimization of a thermoelectric generator for automotive application using an improved whale optimization algorithm," *Sustainable Energy Fuels*, vol. 7, no. 23, pp. 5528–5545, 2023.
[30] C. Wu and W. Schulden, "Specific heating load of thermoelectric heat pumps," *Energy Conversion and Management*, vol. 35, no. 6, pp. 459–464, 1994.
[31] X. Gou, H. Xiao, and S. Yang, "Modeling, Experimental study and optimization on low-temperature waste heat thermoelectric generator system," *Applied Energy*, vol. 87, no. 10, pp. 3131–3136, 2010.